Scripta METALLURGICA et MATERIALIA
Vol. 25, pp. 1011-1016, 1991
Printed in the U.S.A.

VIEWPOINT SET No. 16

DEBOND MECHANICS OF BRITTLE MATERIALS

Z. Suo
Mechanical Engineering Department, University of California, Santa Barbara, CA 93106, USA

(Received December 4, 1990)
(Revised February 27, 1991)

1. Introduction

I shall sketch the elements of the pragmatic theory of interface fracture, and the particular problems that have been stimulating. The two sections at the end update several topics of the current research. The development in the last five years has been driven by the increasing recognition of the roles of interfaces in engineered materials. For ceramic-matrix composites, moderately weak matrix-fiber interfaces, allowing debond and pull-out, enhances the overall toughness. On the other hand, strong bonding is a prerequisite to the performance of layered electronic and structural materials. Mechanics issues are: how the debond resistance can be measured, why microstructures control the debond resistance, and if the interface does debond, what will be the consequences.

Efforts had been made to quantify the bond adhesion long before the advent of the fracture mechanics. Peeling force, for example, is commonly used to determine the adherence of tapes to substrates. Wetting angles and bond strength are other examples. These properties are indicative, but not quantitatively useful in the designs for controlled debond. After the initial success of the Irwin's stress intensity factors, Williams, in a series of studies on the notch singularities, discovered the oscillatory field around an interface crack tip (1). The conceptual difficulties, the stress oscillation and crack face penetration, delayed the progress. Apart from analytic papers by several eminent scholars, the field was largely dormant until the mid-eighties.

In search of techniques to screen the fiber coatings for brittle composites, Evans and his coworkers (2) initiated a pragmatic approach to the subject. The debond resistance is determined experimentally as the critical energy release rate at various mode mixities. Rice (3) pointed out that, on the basis of the small-scale contact, the oscillatory singularity does *not* contradict with the notions of fracture mechanics. Further, the singularity prompts an unambiguous definition of the mode mixity. In fact, the interface fracture mechanics parallel almost all aspects of the mixed mode fracture mechanics of homogeneous materials. The subject has been advanced by Hutchinson and Suo (4) in the comprehensive study of cracks in layered materials. More recently, extensions are made to anisotropic materials, piezoelectrics, and dynamic debonding. A systematic approach emerges to treat the large-scale-bridging and large-scale-contact.

2. Energy Accounting

Griffith's energy accounting defines the *debond driving force*. Consider a homogeneous, nonlinear, elastic material with a strain energy function, w, defined by

$$\dot{w} = \sigma_{ij}\dot{\gamma}_{ij} \tag{2.1}$$

where σ is the stress, γ the strain, and the superimposed dot means *an increment of*. Now two such materials are bonded, with a debonding area A. The system is loaded by a generalized force P and the associated displacement Δ. The strain energy in the body, U, accumulates such that

$$\dot{U} = P\dot{\Delta} - \mathcal{G}\dot{A} \tag{2.2}$$

Analogous to P that drives Δ, the equation defines $\mathcal{G}$ as the driving force for the debonding area. If Δ is maintained by the grips, $\mathcal{G}$ is the strain energy *decrease* to create a unit debond area. Load-maintained systems can be treated with the complimentary energy, $U^c = P\Delta - U$. A Legendre's transformation modifies (2.2) and gives

$$\dot{U}^c = \Delta\dot{P} + \mathcal{G}\dot{A} \tag{2.3}$$

Thus, $\mathcal{G}$ is the complementary energy *increase* to create a unit debond area if P is fixed. Consistent with (2.2) and

0036-9748/91 $3.00 + .00

(2.3), $\mathcal{G}$ can be rewritten as

$$\mathcal{G} = -(\partial U / \partial A)_{\Delta} = (\partial U^c / \partial A)_P \tag{2.4}$$

For a bimaterial with the interface along the x-axis, with the displacement and traction continuous across the interface, the Rice's J-integral (5)

$$J = \int (w n_x - n_i \sigma_{ip} \partial u_p / \partial x) ds \tag{2.5}$$

vanishes over contours not enclosing any singularity. The energy release rate $\mathcal{G}$ equals the J-integral over any path that begins at a point on the lower crack face and ends at another point on the upper crack face. In general, the driving force is obtained with numerical stress analysis. But for the practical problems to be described, rudimentary mechanics suffice.

Fiber pull-out has been modeled at various levels of sophistication; see (6) for the background. Consider a fiber being pulled out from an infinite matrix (Fig. 1). The energy stored in the fiber can be estimated as if the fiber were clamped at the debond front. Thus,

$$U^c = \pi R^2 a \sigma^2 / 2E \tag{2.6}$$

where R is the fiber radius, a the debond length, E the Young's modulus of the fiber, and σ the pull-out stress. Note the debond area is $A = 2\pi Ra$; the differentiation (2.4) gives

$$\mathcal{G} = R\sigma^2 / 4E \tag{2.7}$$

The estimate, which ignores the compliance at the fiber-matrix junction, is accurate when the debond length exceeds the fiber diameter.

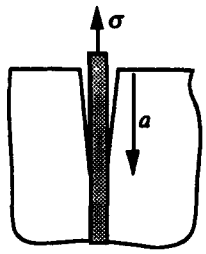

Fig. 1 Axial-section of fiber pull-out.

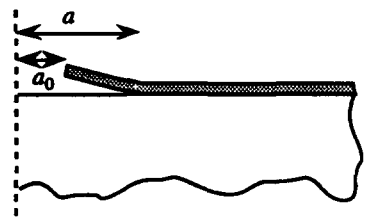

Fig. 2 Axial-section of a thin film debonding from a hole.

Thin film cracking of many patterns has inspired a new problem area (4). Figure 2 illustrates a debond emanating from the edge of a hole in a pre-tensioned film. The energy release rate is (7)

$$\mathcal{G} = \frac{2hE\varepsilon_0^2}{1-\nu^2}\left[1 + \frac{1-\nu}{1+\nu}\left(\frac{a}{a_0}\right)^2\right]^{-2} \tag{2.8}$$

where ε_0 is the mismatch strain between the film and substrate, h the film thickness, a_0 the hole radius, a the debond radius, E and ν the Young's modulus and the Poisson's ratio of the film. Debond from a hole is stable: $\mathcal{G}$ decreases as the crack extends. It has been used to determine the interface toughness, and is particularly feasible when either the film or substrate is transparent, so that the decohesion radius a can be readily measured. For a given material combination, the debond resistance, mismatch strain and elastic parameters are fixed. Thus, the thinner the film, the smaller the decohesion will be. Debond can be practically suppressed if the film is sufficiently thin. The existence of a critical fail-safe thickness is characteristic of most cracking patterns in layered materials.

Adhesive joints have played a special role in the development of the interfacial fracture mechanics. Debond resistance for many systems are determined using sandwiches consisting of a thin layer bonded between two identical substrates (Fig. 3). If the layer thickness is small compared with the overall specimen size, the remote stress field is not perturbed by the layer, but controlled by the regular stress intensity factors, K_I^{∞} and K_{II}^{∞}, reduced from the applied load as if the specimen were entirely homogeneous. The J-integral conservation requires the debond driving force to be

$$\mathcal{G} = \left(K_I^{\infty 2} + K_{II}^{\infty 2}\right)\left(1-\nu^2\right) / E \tag{2.9}$$

where the elastic constants are for substrates. The elastic constants of the layer do not affect the driving force, nor does the residual stress in the layer, induced inevitably during the bonding. However, the elastic mismatch between the layer and the substrates breaks the local symmetry, leading to a phase shift between the local field and the remote loading (4).

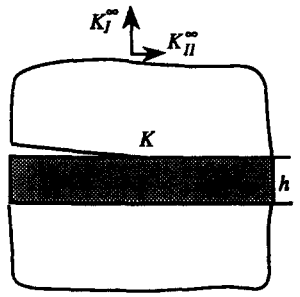

Fig. 3 A sandwich with an interface crack

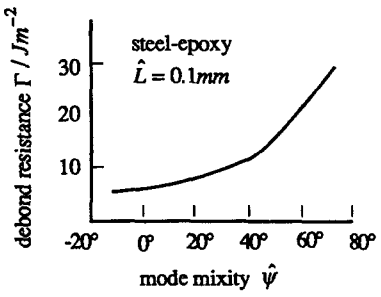

Fig. 4 Debond resistance vs. mode mixity.

Debond resistance is defined as the critical driving force at the onset of propagation:

$$\mathcal{G}_{critical} \equiv \Gamma(\hat{\psi}) \tag{2.10}$$

The resistance Γ depends on the mode mixity $\hat{\psi}$, as noted. The mode mixity measures the ratio of shearing to opening stresses on the interface, and a precise definition will be in the next section. Obviously, Γ depends on other factors, *e.g.*, the bonding process and environment. Diffusion bonded ceramic substrates have different debond resistance from those bonded with an adhesive. Debond resistance over large range of mode mixity has been measured for model systems (8-11). The experimental curve for a steel-epoxy interface (9) is sketched in Fig. 4. Observe that Γ indeed varies with the mode mixity, and increases as the mode changes form predominantly opening to predominantly shear.

3. Williams' Singularity

This section collects mathematical details that underlie the concepts of mode mixity and K-annulus. As the interface crack tip is approached, the stresses asymptote to (1)

$$\sigma_{ij}(r,\theta) = \mathrm{Re}\left[Kr^{i\varepsilon}\right](2\pi r)^{-1/2}\Sigma_{ij}^1(\theta) + \mathrm{Im}\left[Kr^{i\varepsilon}\right](2\pi r)^{-1/2}\Sigma_{ij}^2(\theta) \tag{3.1}$$

where (r, θ) is the polar coordinate centered at the crack tip, and $r^{i\varepsilon} = e^{i\varepsilon \ln r} = \cos(\varepsilon \ln r) + i\sin(\varepsilon \ln r)$. The angular functions, Σ_{ij}^1 and Σ_{ij}^2, depending on ε, are listed in (12). The *oscillation index* is given by

$$\varepsilon = \frac{1}{2\pi}\ln\left[\frac{(3-4\nu_1)/\mu_1 + 1/\mu_2}{(3-4\nu_2)/\mu_2 + 1/\mu_1}\right] \tag{3.2}$$

where μ and ν are the shear modulus and Poisson's ratio, and the subscripts distinguish the two materials. The bielastic constant is bounded within $|\varepsilon| < (1/2\pi)\ln 3 \approx 0.175$. The complex stress intensity factor K scales the singularity, such that the interface traction asymptotes to

$$\sigma_y + i\tau_{xy} = Kr^{i\varepsilon}(2\pi r)^{-1/2} \tag{3.3}$$

and the crack face displacements to

$$\delta_y + i\delta_x = \left(\frac{1-\nu_1}{\mu_1} + \frac{1-\nu_2}{\mu_2}\right)\frac{Kr^{i\varepsilon}(2r/\pi)^{1/2}}{(1+2i\varepsilon)\cosh(\pi\varepsilon)} \tag{3.4}$$

An Irwin-type relation connects $\mathcal{G}$ and the amplitude of K:

$$\mathcal{G} = \frac{1}{4}\left(\frac{1-\nu_1}{\mu_1} + \frac{1-\nu_2}{\mu_2}\right)\frac{|K|^2}{\cosh^2(\pi\varepsilon)} \tag{3.5}$$

Except for K, the near tip filed is independent of the external geometry and loading.

The *mode mixity* $\hat{\psi}$ can also be specified using K. Let $\hat{L}$ be an *arbitrary* length, and define $\hat{\psi}$ as

$$K\hat{L}^{i\varepsilon} = |K| \exp(i\hat{\psi}) \tag{3.6}$$

A physical interpretation follows. The interface traction is now

$$\sigma_y = |K|(2\pi r)^{-1/2} \cos\left[\hat{\psi} + \varepsilon \ln(r/\hat{L})\right], \quad \tau_{xy} = |K|(2\pi r)^{-1/2} \sin\left[\hat{\psi} + \varepsilon \ln(r/\hat{L})\right] \tag{3.7}$$

The stresses oscillate with r; $\hat{\psi}$ is the traction phase at $r = \hat{L}$:

$$\tan\hat{\psi} = \tau_{xy} / \sigma_y \tag{3.8}$$

The length $\hat{L}$ may be chosen to correspond to some process zone size. But it need not be, so long as it is reported with the experimental data, as done in Fig. 4. As implied by (3.6), for two lengths, the mode mixity shifts by

$$\hat{\psi}_2 - \hat{\psi}_1 = \varepsilon \ln(\hat{L}_2 / \hat{L}_1) \tag{3.9}$$

For the steel-epoxy interface, $\varepsilon = 0.08$; the length ratio $\hat{L}_2 / \hat{L}_1 = 100$ will cause the shift $\hat{\psi}_2 - \hat{\psi}_1 \approx 20°$. Thus, in Fig. 4, the choice $\hat{L}$ = 10 mm, instead of $\hat{L}$ = 0.1 mm, would translate the curve by 20°. One may think of $\hat{\psi}$ as a relative measure of the mode mixity, analogous to the Fahrenheit as a measure of the temperature, the origin and scale chosen with a convention.

Specimen calibrations are cataloged in (4). Given a debond specimen of size L loaded by stress σ, dimensionality and linearity dictate

$$K = Y \exp(i\psi) \sigma L^{1/2 - i\varepsilon} \tag{3.10}$$

The real numbers Y (> 0) and ψ depend on the dimensionless parameters of the specimen, and can be evaluated with a stress analysis. With K in hand, $\mathcal{G}$ is given by (3.5), and the mode mixity by

$$\hat{\psi} = \psi + \varepsilon \ln(\hat{L} / L) \tag{3.11}$$

For similar geometries with different sizes L_1 and L_2, ψ is the same, but the mode mixities differ by

$$\hat{\psi}_2 - \hat{\psi}_1 = -\varepsilon \ln(L_2 / L_1) \tag{3.12}$$

This is *not* an artifact: it says that the stress ratio (3.8) at $r = \hat{L}$ varies with the specimen size.

4. K-Annulus: Yielding, Contact, Bridging

In the above, each solid is assumed to be homogeneous and linearly elastic, the interface a smooth two dimensional object, and the crack faces traction-free. These assumptions can hardly be satisfied in practice. In addition, the crack tip field must be perturbed by the specimen geometry and loading distribution. These considerations lead to the notion of K-annulus. If the size of all the *irregularities* is small compared with the smallest length of the specimen, owing to the square root singularity, the Williams' field is still approximately unperturbed within an *annulus* larger than the irregularity size, but smaller than the external geometry. Consequently, the debond resistance $\Gamma(\hat{\psi})$ is justified to be material specific, independent of the geometry and size of the specimen. The debond resistance is specimen dependent if the irregularity scale becomes comparable to the specimen size. Yielding, contact and bridging are practically significant; their implications are summarized below.

The *small-scale-yielding* requirements set a lower bound to the size of the specimens acceptable for the linear fracture mechanics. For an isolated interface crack tip, the plastic zone size is (13)

$$r_p = (0.1 \sim 0.6)(|K|/\sigma_0)^2 \tag{4.1}$$

where σ_0 is the lower yield stress of the substrates, and the prefactor increases with the mode mixity. In practice, r_p is required to be a fraction of the specimen size. Thus, tougher interfaces must be tested using larger specimens.

The *small-scale-contact* requirements set the interval of the mode mixity. From (3.4), the crack opening is

$$\delta_y = \delta \cos\left[\hat{\psi} + \varepsilon \ln(\hat{L}/r) - \tan^{-1}(2\varepsilon)\right] \tag{4.2}$$

where δ is the magnitude of the total displacement jump. If $\hat{L}$ is interpreted as the process zone size, and if $\delta_y > 0$

is required within the K-annulus, say $\hat{L} < r < 100\hat{L}$, the mode mixity must be confined within

$$-\pi/2+2\varepsilon < \hat{\psi} < \pi/2-2.6\varepsilon, \quad \varepsilon > 0$$

$$-\pi/2-2.6\varepsilon < \hat{\psi} < \pi/2+2\varepsilon, \quad \varepsilon < 0 \tag{4.3}$$

The number 100 is arbitrary, but the near tip fields must give way to the external boundary conditions when r exceeds some multiple of $\hat{L}$.

Large-scale-contact prevails in some technical problems. Figure 5 illustrates a few: the frictional sliding in the fiber pull-out due to residual compression or fiber asperity, wear delamination of protective coatings, and internal debonding of layered materials. The crack tip experiences predominantly shear, and the friction shields the driving force. Dugdale models can be used to analyze these (6).

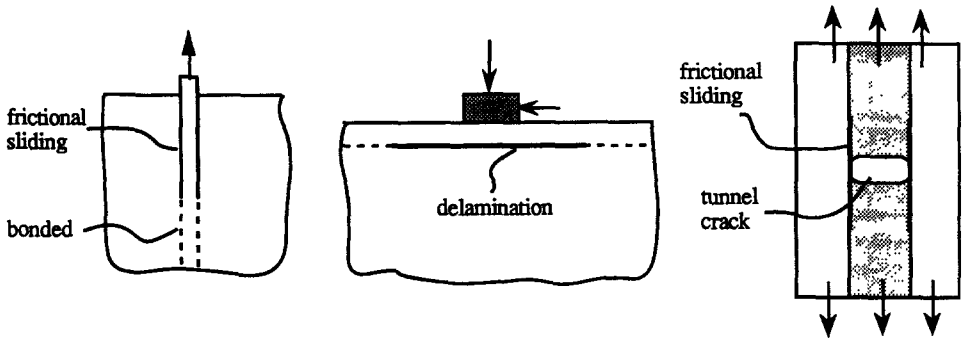

a) Fiber pull-out b) Wear delamination of a coating c) Internal debonding

Fig. 5 Examples of large scale contact.

Large-scale-bridging appears either because the microstructure is large (as for composites), or because the characteristic specimen size is small (as for craze debond of polymer coatings); see (14) for the literature review. Suppose the bridging response is described by a potential $\phi(\delta_y, \delta_x)$, such that

$$\dot{\phi} = \sigma_y \dot{\delta}_y + \tau_{xy} \dot{\delta}_x; \quad \phi(0,0) = 0 \tag{4.4}$$

where σ_y and τ_{xy} are tractions opposing the debond. An application of the J-integral shows

$$\mathcal{G}_R = \mathcal{G}_0 + \phi(\tilde{\delta}_y, \tilde{\delta}_x) \tag{4.5}$$

where $\mathcal{G}_R$ is the J-integral over the external boundary of the specimen, $\mathcal{G}_0$ is the debond driving force at the crack tip, and $\tilde{\delta}_y$, $\tilde{\delta}_x$ are opening and sliding at the end of the bridging zone. For delamination in layered materials, the damage zone is typically large compared with the ply thickness, but still small compared with the lateral dimension. For this situation, $\mathcal{G}_R$ is independent of the damage law. If in addition the debond resistance at the crack tip, $\mathcal{G}_0$, is a constant independent of the mode mixity, equation (4.5) suggests a method to determine the bridging response directly from the experimental R-curves (14). Since the overall fracture resistance now depends on the specimen geometry, we favor to regard the bridging response as the basic material properties. Once the bridging response is determined experimentally, any arbitrary geometry can be analyzed numerically.

5. Anisotropy, Dynamics, Piezoelectrics

Anisotropic Solids have been studied by several authors; see (15) for the literature review. The debond resistance can still be defined as the critical debond driving force. But the singularity structure is more involved, which in turn complicates the mode mixity specification. Nonetheless, the near tip field still consists of two types of singularities: $r^{-1/2}$ and $r^{-1/2\pm i\varepsilon}$. For example, for orthotropic bimaterials, the principal axes aligned with the interfaces and the crack front normal to the principal plane, the interface traction ahead the crack tip is

$$\sigma_y + i\tau_{xy} / \eta = Kr^{i\varepsilon}(2\pi r)^{-1/2} \tag{5.1}$$

where K is the complex stress intensity factor, and η depends on elastic constants. Mode mixity specification based on this is discussed in (16). Mixed mode delamination in cross-plies has been analyzed (17).

Dynamic Debonding is examined in the light of the pragmatic approach (18). Griffith's accounting now must include the kinetic energy T of the body:

$$\dot{U} + \dot{T} = P\dot{\Delta} - \mathcal{G}\dot{A} \tag{5.2}$$

Here the superimposed dots mean the time rates. Under arbitrary dynamic loading and crack motion, at any instance, the crack tip experiences a two dimensional, steady-state singularity. The singularity has a structure similar to (5.1) even for isotropic bimaterials, with η now dependent on the instantaneous crack speed.

Piezoelectrics produce electric fields when stressed, and undergo deformation when charged. The advanced piezoelectric ceramics are commonly layered with other materials, or embedded in polymer matrices (19). A comprehensive study has been carried out for cracks in piezoelectrics, and on debond along the interfaces between piezoelectrics and other materials (20). Griffith's accounting should include energy change due both to deformation and polarization. Four modes of square root singularities prevail at the crack tip in homogeneous piezoelectrics. For interface cracks, a new type of singularity is discovered. Specifically, the singularities form two pairs. One pair is the usual oscillatory singularity $r^{-1/2\pm i\varepsilon}$, and the other pair is real and of the form $r^{-1/2\pm\kappa}$, where ε and κ are real numbers depending on the constitutive constants. A collection of boundary value problems has been solved, including the generalized Griffith's crack problem.

Acknowledgements - The work is supported by ONR/URI contract N-0-0014-86-K-0753, and by NSF grant MSS-9011571.

References

1. M.L. Williams, *Bull. Seismol. Soc. Am.*, **49**, 199 (1959).
2. A.G. Evans, M. Ruhle, B.J. Dalgleish, P.G. Charalambides, *Mater. Sci. Eng.*, **A126**, 53 (1990).
3. J.R. Rice, *J. Appl. Mech.* **55**, 98 (1988).
4. J.W. Hutchinson and Z. Suo, "Mixed mode cracking in layered materials". *Advances in Applied Mechanics*, **28**. Academic Press, New York (1991). In the press
5. J.R. Rice, *J. Appl. Mech.* **35**, 379 (1968).
6. J.W. Hutchinson and H.M. Jensen, "Models of fiber debonding and pullout in brittle composites with friction". Submitted for publication.
7. R.J. Farris and C.L. Bauer, *J. Adhesion*, **26**, 293 (1988).
8. H.C. Cao and A.G. Evans, *Mech. Mater.*, **7**, 295 (1989).
9. J.S. Wang and Z. Suo, *Acta Met.*, **38**, 1279 (1990).
10. M.D. Thouless, *Acta Met.*, **38**, 1135 (1990).
11. K.M. Liechti and Y.-S. Chai, "Biaxial loading experiments for determining interfacial toughness". *J. Appl. Mech.* In the press.
12. J.R. Rice, Z. Suo and J.S. Wang, in *Metal-Ceramic Interfaces*, Eds. M. Ruhle, A.G. Evans, M.F. Ashby and J.P. Hirth, Pergamon Press, New York, 269 (1990).
13. C.F. Shih, and R.J. Asaro, *J. Appl. Mech.* **55**, 299 (1988).
14 Z. Suo, G. Bao and B. Fan, "Delamination *R*-curve phenomena due to damage". *J. Mech. Phys. Solids.* In the press.
15. Z. Suo, *Proc. R. Soc. Lond.* **A427**, 331 (1990).
16. T.C. Wang, C.F. Shih and Z. Suo, "Crack extension and kinking in laminates and bicrystals". *Int. J. Solids Structures.* In the press.
17. H.C. Choi, C.F. Shih and Z. Suo, "Specimens to determine mixed mode delamination toughness for cross-ply laminates". Work in progress.
18. W. Yang, Z. Suo and C. F. Shih, "Mechanics of dynamic debonding". *Proc. Roy. Soc. Lond.* In the press.
19. R.C. Pohanka, and P.L. Smith, in *Electronic Ceramics, Properties, Devices and Applications*. Ed. L.M. Levinson. Marcel Dekker, Inc. New York.
20. Z. Suo, C.-M. Kuo, D.M. Barnett and J.R. Willis, "Cracking and debonding of piezoelectric ceramics". Submitted to *J. Mech. Phys. Solids.*